New method for monitoring soil water infiltration rates applied to a disc infiltrometer

David Moret-Fernández[a] [*], César González-Cebollada[b]

[a] *Departamento de Suelo y Agua Estación Experimental de Aula Dei Consejo Superior de Investigaciones Científicas (CSIC). PO Box 202, 50080, Zaragoza, Spain.*

[b] *Área de Mecánica de Fluidos. Escuela Politécnica Superior de Huesca - Universidad de Zaragoza. Carretera de Cuarte s/n. 22071, Huesca, Spain.*

* Corresponding author.

Telf: +34 976 71 61 40

Fax: +34 976 71 61 45

E-mail address: david@eead.csic.es

New method for monitoring soil water infiltration rates applied to a disc infiltrometer

Abstract

Disc infiltrometers commonly use low-capacity water-supply reservoirs made of small-diameter tubes. This reservoir geometry allows accurate measurements of water levels, but makes it necessary to stop the infiltration measurements to refill the water-supply reservoir when long-term infiltration experiments are conducted. The purpose of this study is to determine if a double Mariotte system provides accurate infiltration rate data from disc infiltrometer. To this end, infiltration rates (*Q*) is calculated from the head losses (ΔH_T) produced by the water flowing along a flexible silicone pipe that connects a high-capacity water-supply reservoir and the disc of the infiltrometer. The method was calibrated in the laboratory using 2- and 3-mm internal-diameter (i.d.) and 50- and 100-cm-long silicone pipes by comparing the measured ΔH_T with the corresponding theoretical values, for different *Q* measured from the drop in water level in the water-supply reservoir. This method was next applied to field conditions, where the infiltration rates (at four supply pressure heads in five different soils) measured from the water-level drop in the water-supply reservoir of a double Mariotte disc infiltrometer (using 2- and 3-mm-i.d. and 100-cm-long silicone pipes) were compared with the corresponding values calculated from ΔH_T measured in the Mariotte tube. An excellent correlation was found in the laboratory experiment between the calculated and the measured ΔH_T ($r^2 = 0.99$), and between *Q* measured from the water-supply reservoir and that calculated from the measured ΔH_T ($r^2 = 0.99$). In the field experiments, excellent correlation was shown between the infiltration rates measured from the water-level drop in the water-supply reservoir and the corresponding values calculated from the ΔH_T measured in the

Mariotte tube. This correspondence indicated that this method would be a consistent alternative to the standard procedure used in the disc infiltrometry technique.

Keywords: Disc infiltrometer; Infiltration rate; Water head losses; Pressure transducers

1. Introduction

The disc infiltrometer (Perroux and White, 1988) has become a very popular instrument for estimations of soil hydraulic properties at the near-zero soil water pressure head. The relatively rapid and portable nature of this technique and its easy applicability in situ makes the disc infiltrometer a very valuable tool in many hydrological and soil science studies. Soil hydraulic properties such as hydraulic conductivity (*K*) sorptivity (*S*) (White et al., 1992), and the size and number of the soil's macro- and meso- water-conductive pores (Moret and Arrúe, 2007) are commonly calculated from the cumulative water-infiltration curves measured with the disc infiltrometer.

Typically, this instrument consists of three parts made of Plexiglass: a base-disc covered by a nylon cloth, a graduated reservoir that provides the water supply, and a bubble tower with a moveable air–entry tube that imposes the pressure head of the water at the cloth base (Angulo-Jaramillo et al., 2000). Commonly, the water-supply reservoir consists of a low-water-capacity clear plastic tube of small diameter, which makes it possible to reduce the infiltrometer weight on the soil surface, and allows for more accurate measurements of water-level changes in the tube. However, this reservoir geometry has the limitation that it results in interruptions of the infiltration measurements to refill the water-supply reservoir when long-term infiltration experiments (i.e. infiltration at successive supply pressure heads at the same sampling point) are performed.

Cumulative soil water infiltration curves obtained with disc infiltrometers are commonly measured by visually noting, at constant intervals of time, the drop in water level in the water-supply reservoir. This method, however, is time-consuming and can lead to errors in water-level measurements due to reader distractions when long-time infiltration samplings are performed. This limitation was satisfactorily solved by Ankeny et al. (1988) and Casey and Derby (2002), who monitored drops in the water level by incorporating two gage transducers or a single differential transducer in the water-supply reservoir, respectively. Similarly, Moret et al. (2004) developed an automated method to measure the changes in water level in the water-supply reservoir by means of a long three-rod coated Time Domain Reflectometry (TDR) probe vertically inserted in the water-supply reservoir.

Other advances in disc infiltrometry technique have addressed new designs in which the disc has been separated from the water-supply reservoir and the bubble tower (Casey and Derby, 2002; Moret and Arrúe, 2005). This reduces the weight of the infiltrometer on the soil surface, reduces the risk of macrostructure collapse when applied on unstructured or freshly tilled soils (Moret and Arrúe, 2005) and consequently results in more accurate estimations of the actual soil hydraulic properties.

The objective of this study is to present an alternative procedure and experimental set-up for disc infiltrometry: a double Mariotte system method which makes it possible to calculate infiltration rates from the head losses produced by the water flowing along a flexible silicone pipe that connects a high-capacity water-supply reservoir and the disc of the infiltrometer. The method was calibrated in the laboratory using 2- and 3-mm internal diameter (i.d.) and 50- and 100-cm-long silicone pipes, and subsequently tested in five field experiments for measuring infiltration rates at different supply water pressure heads.

2. Theory

An incompressible fluid moving along a circular pipe can be described by the Bernoulli equation (Giles et al. 1994). When there is no energy input, this equation is

$$\frac{V_1^2}{2g}+\frac{P_1}{\gamma}+Z_1=\frac{V_2^2}{2g}+\frac{P_2}{\gamma}+Z_2+\Delta H_T \quad (1)$$

where V_i (m s^{-1}), Z_i (m) and P_i (kg·m^{-1}·s^{-2}) are the average flow velocity, the elevation in the direction of gravity from a reference level, and the pressure at point *i*, respectively. The *g* (m s^{-2}) parameter is the acceleration due to gravity; γ (kg·m^{-2}·s^{-2}) is the specific weight of the fluid, defined as density (kg·m^{-3}) multiplied by *g*; and ΔH_T (m) is the total head losses produced by the friction of the fluid moving through the pipe. Considering two reservoirs connected with a pipe of length *L* and diameter *D* (Fig. 1), the head losses produced between points one and two, when the fluid flows from the right to the left reservoir, can be approached from Eq. (1) according to

$$\Delta H_T = h_B - h_{B'} \quad (2)$$

where h_i is the difference in height between the B and the B' points shown in Fig. 1.

The total head losses, ΔH_T, in the system can be calculated according to

$$\Delta H_T = \Delta H_C + \sum_1^n \Delta H_{s\_i} \quad (3)$$

where ΔH_C is the continuous head loss produced by the water flowing along the tube and ΔH_{s_i} is the singular head loss which corresponds to the head losses produced by necks or constrictions in the pipes, or by other singularities.

The ΔH_C is described by the Darcy-Weisbach (Giles et al., 1994) equation according to

$$\Delta H_C = f\left(\mathrm{Re},\frac{\varepsilon}{D}\right)\cdot\frac{L}{D}\cdot\frac{V^2}{2g} \quad (4)$$

where *f* is the friction coefficient, ε is the pipe roughness (m), D is the pipe diameter (m), L is the pipe length (m) and Re is the Reynolds number defined as

$$\mathrm{Re}=\frac{VD}{\nu} \quad (5)$$

where ν is the kinematic viscosity (m^2 s^{-1}) of the fluid. The relationship between the water temperature, *t* (ºC), and the kinematic viscosity of water can be described according to the empirical equation (r^2 = 0.99) obtained from the table in Giles et al. (1994) for the usual values of *t*,

$$\nu = 6.95 \cdot 10^{-10} t^2 - 5.31 \cdot 10^{-8} t + 1.78 \cdot 10^{-6} \quad (6)$$

Considering that the friction coefficient for a laminar flow (Re < 2000) is given by

$$f = \frac{64}{\mathrm{Re}} \quad (7)$$

and the water flow, *Q*, through a circular pipe is expressed by

$$Q = V\pi \left(\frac{D}{2} \right)^2 \quad (8)$$

the ΔH_C along the pipe for a laminar water flow (Eq. 7) can be expressed as

$$\Delta H_C = \frac{128\nu}{\pi g} \frac{QL}{D^4} \quad (9)$$

Equation (9) is the Poiseuille equation and shows the linear relationship between flow rate and linear head losses in a laminar flow of an incompressible fluid.

The singular head loss, ΔH_S, (Giles et al., 1994) is expressed according to

$$\Delta H_S = K_S \frac{V^2}{2g} = K \frac{8Q^2}{\pi^2 g D^4} \quad (10)$$

where K_S is a constant depending on the pipe singularity.

Applying Eqs. (9) and (10) to Eq. (3) we obtain

$$\Delta H_T = Q \frac{128\nu}{\pi g} \frac{L}{D^4} + Q^2 \frac{8}{\pi^2 g D^4} \left(\sum_1^n K_{Si} \right) \quad (11)$$

Solving Eq. (11), we finally obtain that the water flow as a function of the total head losses can be expressed as

$$Q = \frac{-\frac{128\nu L}{\pi g D^4} + \left[\left(\frac{128\nu L}{\pi g D^4} \right)^2 + \frac{32\Delta H_T \left(\sum_i^n K_{Si} \right)}{g\pi^2 D^4} \right]^{1/2}}{\frac{16\left(\sum_1^n K_{Si} \right)}{g\pi^2 D^4}} \qquad (12)$$

3. Material and methods

3.1. Calibration of the silicone pipe head losses

A first laboratory experiment was performed to determine the relationship between the water flow (Q) through a pipe and the total head losses (ΔH_T). The experimental design consisted of a double Mariotte system with two silicone pipes (defined as 100 cm length and 3- and 2-mm i.d., respectively) that connected the base of a water-supply reservoir (a clear plastic tube of 75 cm height and 5 cm i.d.) with the base of a Mariotte tube (a clear plastic tube of 35 cm height and 2.5 cm i.d.), and a third silicone pipe of 3 mm i.d. and 150 cm length that connected the top of the Mariotte tube with a hole made at 25 cm height in the water-supply reservoir (Fig. 1). The water outlet and air inlet in the double Mariotte system were made through two silicone pipes (3 mm i.d.) inserted in the base and at 3 cm height above the water outlet tube in the Mariotte tube, respectively (Fig. 1). The real geometries of the water-flow silicone pipes (effective length and i.d.) used in the laboratory and the subsequent field experiments are summarized in Table 1. The effective i.d. of the 3-mm and 2-mm silicone pipes were measured from the effective length of the pipes and the water volume contained in the respective pipes. The K_S values for the singular head loss (ΔH_S) ranged between 0.3 and 1 (Giles et al., 1994), depending on the different constrictions or necks observed along the silicone pipe connecting the water-supply reservoir and the Mariotte tube (Fig. 1).

Under static conditions, the water level in the Mariotte tube is defined by the height of the air-inlet tube in the water-supply reservoir. However, under dynamics conditions, when the water flows from the water-supply reservoir out of the system, the water level in the Mariotte tube will fall as a function of the Q flowing through the silicone pipe (Fig. 1). The water level in the double Mariotte system was monitored with two ±1 psi differential pressure transducers (PT) (model 26PCDFA6D, Microswitch, Honeywell) which, connected to a datalogger (CR1000 Campbell Scientific Inc.), were inserted at the bottom of the Mariotte tube and the water-supply reservoir, respectively (Casey and Derby, 2002). The ΔH_T was also determined by visually noting the water level in the Mariotte tube. The different Q were regulated by the difference in height between the air inlet and water outlet in the Mariotte tube (Fig. 1). Seven different Q for the 3-mm i.d. silicone pipes (from 0.6 to 8.0 L h^{-1}) and four different Q for the 2-mm i.d. silicone pipes (from 0.5 to 2.5 L h^{-1}), monitored from the drop in water level in the water-supply reservoir, were used to determine the relationship between the theoretical ΔH_T (Eq. 11) and the water level measured in the Mariotte tube. The comparison between the theoretical and experimental ΔH_T was replicated twice for each value of Q. The water temperature was measured at real time with a thermistor which, connected to the datalogger, was installed at the bottom of the water-supply reservoir. This same experiment was again repeated using 50-cm-long silicone pipes of 3- and 2-mm i.d. (Table 1), respectively.

A second laboratory experiment was performed to determine the effect of the silicone pipes on the Mariotte tube water outflow, i.e. to compare water flow from the double Mariotte system with water flow from the single Mariotte tube. The water outflow measured for four different Q (from 0.47 to 4.57 L h^{-1}) using the double Mariotte system (Fig. 1) with closed silicone pipes was compared with the corresponding values measured with the same system when the 2- or 3-mm-i.d and 100-cm-length silicone pipes were opened. The Q, regulated by the difference of height between the air inlet and water outlet in the Mariotte tube, was calculated from the rising water level measured with a PT installed at the bottom of a reservoir (a 45-cm-long and 1.6-cm-i.d. clear plastic tube) that collected the Mariotte tube water outflow.

3.2. Infiltrometer design and field testing

The disc infiltrometer design used to test the method proposed here for measuring infiltration rates from water head losses (patent pending) consists in a double Mariotte system where the three elements of the infiltrometer, the Mariotte tube with the base disc, the water-supply reservoir and the bubble tower, are separate from one another (Fig. 2) (Moret and Arrúe, 2005). The base of the infiltrometer, which is connected to the bubble tower through a 3-mm-i.d. and 100-cm-long silicone pipe, is a 10-cm-diameter disc that has a 35-cm-high, 2.5-cm-i.d. clear plastic tube (Mariotte tube) inserted on top of it. The Mariotte tube is connected to the water-supply reservoir (a 5-cm-i.d. and 80-cm-high clear plastic tube) with three silicone pipes: (1) an air-flow pipe (a 3-mm-i.d. and 200-cm-long silicone pipe) that connects the top of the Mariotte tube with a hole made 25-cm above the bottom of the water-supply reservoir; and (2) 3-mm and 2-mm-i.d., 100-cm-long pipes for flowing water that connect the bottoms of the water-supply reservoir and the Mariotte tube. This configuration makes it possible to obtain two different values of ΔH_T depending on whether the 2-mm or 3-mm i.d. pipes are opened or closed, respectively. The magnitude of the soil water infiltration will decide which one of the water-flow pipes should be opened. For instance, while accurate measurements of ΔH_T for water flows lower than 2 L h^{-1} can be obtained using the 2-mm-i.d. pipe, the 3-mm-i.d. one would be preferable for water flows higher than 2 L h^{-1}. The drops in water level in the Mariotte tube and the water-supply reservoir were automatically monitored using two ±1 psi differential PT (model 26PCDFA6D, Microswitch, Honeywell) which, connected to a datalogger (CR1000, Campbell Scientist Inc.), were inserted at the bottom of the Mariotte tube and water-supply reservoir, respectively (Casey and Derby, 2002). The water temperature during the infiltration experiments was measured with a thermistor which, also connected to the datalogger, was installed at the bottom and inside of the water-supply reservoir (Fig. 2) The temperature measured by this thermistor was used to recalculate the actual kinematic viscosity (Eq. 6), which was subsequently employed to calculate the total head losses (Eq. 12) . A second thermistor, that measured the environment temperature, was used to correct the effect of the temperature on the PT for the water-level measurements, which calibration was performed in a previous laboratory experiment. The K_S values for the singular head losses (Eq. 10) in the disc infiltrometer (Fig. 2) were the same to those used for the laboratory experiment (Fig. 1).

The new infiltrometer design was tested in five soils with different degrees of soil compaction (Table 2). The soil dry bulk density (ρ_b), also used to determine the antecedent volumetric water content of the soil, was determined by the core method with core dimensions of 50 mm diameter and 50 mm height. Core samples were taken the same day as infiltration measurements and near the measurement locations. All the measurements, which were taken on a nearly level area, were performed on the surface layer after removing the surface crust. The base of the infiltrometer disc was covered with a nylon cloth of 20-μm mesh, and in order to ensure good contact between the disc and the soil a thin layer of commercial sand (80–160 μm grain size) was poured onto the soil surface. The initial water level in the Mariotte tube, before starting the infiltration measurements, was obtained by gravity-filling from the water-reservoir the Mariotte tube when both the water-flow pipes were opened and the disc plus Mariotte tube system rested on a plastic bag placed on the sand contact. Once the Mariotte tube water level was stabilised, the plastic bag was removed and the disc was placed on the sand surface to start the infiltration measurements. Four different supply pressure heads (from -10 to 0 cm water head) were used (Table 2), and only infiltration measurements during the steady state water flow were considered. In this case, the cumulative water infiltration was considered in steady state when no changes in the Mariotte tube water level were visually observed. The infiltration rate at the different supply pressure heads measured from the drop in water level in the water-supply reservoir was compared with the corresponding values calculated from ΔH_T (Eq. 12) measured in the Mariotte tube. While the 2-mm-i.d. pipe was used for water flows lower than one bubble every 3 seconds (approximately), the 3-mm-i.d. pipe was chosen for higher water infiltration rates. Table 2 shows the i.d. of the silicone tube used for the infiltration measurement at each tension.

4. Results and discussion

The excellent correlation between the outlet water flow measured with a single Mariotte tube and the corresponding values measured with the double Mariotte system when the 2- or 3-mm-i.d. and 100-cm-long water-flow silicone pipes were opened (Fig. 3) demonstrates that head losses in the silicone pipe do not have any significant effect on the outlet water from the Mariotte tube. As already observed by Casey and Derby (2002) and Madsen and Chandler (2007) in similar infiltrometer designs, Fig. 4, which compares the water level of the Mariotte tube visually measured and monitored by PT, demonstrates that the PT technique applied to the Mariotte tube is an accurate method for monitoring water levels in real time. The Reynolds number (Eq. 5) calculated for the different Q and the four different silicone pipe geometries used in the laboratory experiment (Table 1) was always significantly lower than 2000 (Table 3), which demonstrates that the Q in the silicone pipes always had a laminar flow. An excellent correlation was also observed between the ΔH_T calculated from Eq. (11) for the four silicone pipe geometries (Table 1) and the different Q (Table 3) and the corresponding ΔH_T values visually measured and PT-monitored from the water level in the Mariotte tube (Fig. 5). Despite this good relationship, a slight deviation from the 1:1 line was observed between the theoretical and the measured water head losses for ΔH_T > 16 cm. These differences could be attributed to some small singular losses (i.e. curvatures in the silicone pipes) not included in the model (Eq. 11), which could have a significant influence on ΔH_T when high water flows are used. The quadratic relationship between ΔH_S and Q (Eq. 10) may explain the phenomenon that small singular losses not included in the model may have a more significant effect on ΔH_T at high values of water flows. The changes in water level in the Mariotte tube measured with the PT after starting the different Q increments through the silicone pipes showed that the double Mariotte system needs some minutes to stabilize the final water-level and thus also ΔH_T value in the Mariotte tube (Fig. 6). The time for water-level stabilization tended to increase with increasing water flows or decreasing i.d. of the pipes (Fig. 6). This would indicate that the stabilization time for the water level in the Mariotte tube would be proportionally related to the total water head losses. The good correlation observed in the laboratory experiment between the Q measured from the water-level drop in the water-supply reservoir and those values calculated from the water level in the Mariotte tube (Eq. 12) (Fig. 7) demonstrate that the latter could be a promising method for measurement of infiltration rates using the disc infiltrometry technique. As observed in Fig. 5 and also in Fig. 7, a slight deviation from the 1:1 line was found for Q > 6 L h^{-}1. These differences, however, can be ignored for a common field application using disc infiltrometers, since numerous field infiltration experiments (e.g. Moret and Arrúe, 2007) have shown that the infiltration rates in soils are usually lower than 5 L h^{-1}. For infiltration rates higher than 8 L h^{-1} (i.e. higher diameter discs or sand columns with Q ranging between 15 and 25 L h^{-1}), the problem associated with the residual head losses at high water flows could be solved by using flexible pipes of higher internal diameter. On the other hand, our results demonstrated that the small i.d. pipes used in this method ensure that the temperature vs. kinematic viscosity dependence (Eq. 6) has a significant influence on the ΔH_C (data not shown) (Eq. 9). This phenomenon means that the water temperature is an important factor to be measured in order to obtain accurate calculations of Q (Eq. 12).

In the field infiltration experiments (Table 2), an excellent correlation (Fig. 8) was found between the infiltration rates measured from the drop in water level in the water-supply reservoir and the corresponding values estimated (Eq. 12) from the water level (ΔH_T) measured in the Mariotte tube of the disc infiltrometer (Fig. 2). The soils used to test this new method of measuring infiltration rates covered a wide range of water flow rates (from 0.046 to 2.22 L h^{-1}) and soil structures (soil dry bulk density ranging between 1.12 and 1.43 g cm^{-3}). We can thus conclude that the method proposed here can be a viable alternative for measuring infiltration rates with disc infiltrometers. In comparison to the conventional method used with the disc infiltrometer, which calculates the soil infiltration rates from the water-level drop in the water-supply reservoir, this new procedure presents some advantages such as:

1. determination of the instantaneous soil water infiltration rate from Eq. (12) by a single notation of the water level in the Mariotte tube (in relation to the air inlet in the reservoir) instead of on the cumulative infiltration as sampled from notations of the falling water table in the water reservoir
2. the use of a high-capacity water-supply reservoir, which allows:
    a. the monitoring of simultaneous infiltrations by using several disc plus Mariotte tube systems connected to a single water-supply reservoir;
    b. long-term infiltration measurements without stopping the experiment to refill the water-supply reservoir;
3. measurement of a wide range of water flows by using water-flow pipes of different i.d.;

However, this new design presents, in comparison to the classical and compacted disc infiltrometer, the disadvantage that needs controlling three independent parts (bubble tower, Mariotte tube, supply reservoir) instead of one as in the original devices. On the other hand, in order to make accurate infiltration rates measurements, the tubing system should be in perfect conditions, (without undesirable constrictions or contamination, e.g. algal growth) since otherwise more negative pressure supply heads will be measured.

5. Conclusions

This paper presents a new procedure which, applied to a disc infiltrometer, allows estimations of infiltration rates by measuring the head losses produced by the water flowing along a silicone pipe. The system, which consists of 2- or 3-mm-i.d. and 100-cm-long silicone pipes that connect a Mariotte tube with a water-supply reservoir, calculates the head losses from the drop in water level that occurs in the Mariotte tube. In the calibration experiment on the laboratory, the measured head losses for a wide range of water flows (from 0.5 to 8.0 $L\ h^{-1}$) were satisfactorily correlated with the corresponding values calculated from hydraulic theory. The field experiments performed to test this method using the new design of disc infiltrometer demonstrate that this procedure is an accurate and consistent alternative to the standard procedures for water-flow measurements commonly used in the disc infiltrometry technique. In particular, this method makes it possible to calculate the instantaneous infiltration rates from simple notations of the head loss and to conduct several simultaneous infiltration discs using a single high-capacity water-supply reservoir. However, new efforts should be made to design an improved disc infiltrometer system that allows simultaneous infiltration measurements at different time steps including the initial transient water infiltration increments and a system for automating the time intervals for changing the supply pressure heads in the bubble tower.

References

Angulo-Jaramillo, R., Vandervaere, J.P., Roulier, S., Thony, J.L., Gaudet, J.P., Vauclin, M., 2000. Field measurement of soil surface hydraulic properties by disc and ring infiltrometers. A review and recent developments. Soil Tillage. Research 55, 1–29.

Ankeny, M.D., Kaspar, T.C., Horton, R., 1988. Design for an automated tension infiltrometer. Soil Science Society of America Journal 52, 893–896.

Casey, F.X.M., Derby, N.E., 2002. Improved design for an automated tension infiltrometer. Soil Science Society of America Journal 66, 64–67.

Giles, R. V., Evett, J. B., Liu, C., 1994. Fluid Mechanics and Hydraulics. Ed. McGraw–Hill Book Company, New York. ISBN 0070205094.

Madsen, M.D., Chandler, D. G., 2007. Automation and use of mini disk infiltrometers. Soil Soil Science Society of America Journal 71, 1469–1472

Moret, D., Arrúe, J.L., 2005. Limitations of tension disc infiltrometers for measuring water flow in freshly tilled soils. In: Faz Cano, A., Ortiz, R., Mermut, A.R. (Eds.), Sustainable Use and Management of Soils. Arid and Semiarid Regions. Advances in Geoecology 36. CATENA- ERLAG Series, Reiskirchen, Germany, pp. 197–204.

Moret, D., López., M.V., Arrúe, J.L., 2004. TDR application for automated water level measurement from Mariotte reservoirs in tension disc infiltrometers. Journal of Hydrology 297**,** 229-235.

Moret, D., Arrúe, J.L., 2007. Characterizing soil water-conducting macro- and mesoporosity as influenced by tillage using tension infiltrometry. Soil Science Society of America Journal 71, 500–506.

Perroux, K.M., White, I., 1988. Designs for disc permeameters. Soil Science Society of America Journal 52, 1205–1215.

White, I., Sully, M.J., Perroux, K.M., 1992. Measurement of surface-soil hydraulic properties: disc permeameters, tension infiltrometers and other techniques. In: Topp, G.C., et al.

(Eds.), Advances in Measurement of Soil Physical Properties: Bringing Theory into Practice. Soil Sci. Soc. Am. Spec. Publ. 30. SSSA, Madisson, WI, pp. 69±103.

Acknowledgements

This research was supported by the Ministerio de Ciencia e Innovación of Spain (grants AGL2007-66320-CO2-02/AGR; 200840I214). The authors are grateful to Darío Testón and Valero Pérez for their help in various technical aspects of this study.

Figure captions

Figure 1. Schematic diagram of the double Mariotte system used in the laboratory experiment to calibrate the water head losses produced by the different silicone pipes shown in Table 1.

Figure 2. Schematic diagram of the disc infiltrometer design used in the field experiments to test the water head losses method for the measurement of the infiltration rates. The K_S are the constant values for the singular head losses in the double Mariotte system.

Figure 3. Relationship between the outlet water flow measured with a single Mariotte tube and the corresponding values measured with the double Mariotte system using the 2- or 3- mm water-flow silicone pipes of 100 cm length.

Figure 4. Relationship between the water level visually measured in a Mariotte tube and the corresponding values monitored using a ±1 psi pressure transducer connected to a datalogger.

Figure 5. Relationship between the total head losses (ΔH_T) calculated from Eq. (11) for the four silicone pipe geometries shown in Table 1 and different water flow rates (Table 3) and the corresponding visual and pressure transducers (PT) values measured from the drop in water level in the Mariotte tube. Regression equations and coefficient of determination (r^2) correspond to the fit for all the PT and visual measured values.

Figure 6. Water-level changes in the Mariotte tube after starting the different water flows through the silicone pipes in (a) the laboratory experiment using the 3-mm-i.d. and 100-cm-long silicone pipe and (b) the field experiment on the freshly mouldboard-tilled loam soil after a pass with a land-roller using the 2- and 3-mm-i.d. silicone pipe of 100-cm length, for the supply tension heads (ψ) shown in Table 2.

Figure 7. Relationship between the water flow values measured in the laboratory experiment from the drop in water level in the water-supply reservoir and those values calculated

by applying to Eq. (12) the water level measured in the Mariotte tube for the four pipe geometries shown in Table 1.

Figure 8. Relationship between the infiltration rates measured in the five field experiments (Table 2) from the drop in water level in the water-supply reservoir and the corresponding values calculated by applying the water level measured in the disc infiltrometer Mariotte tube to Eq. (12).

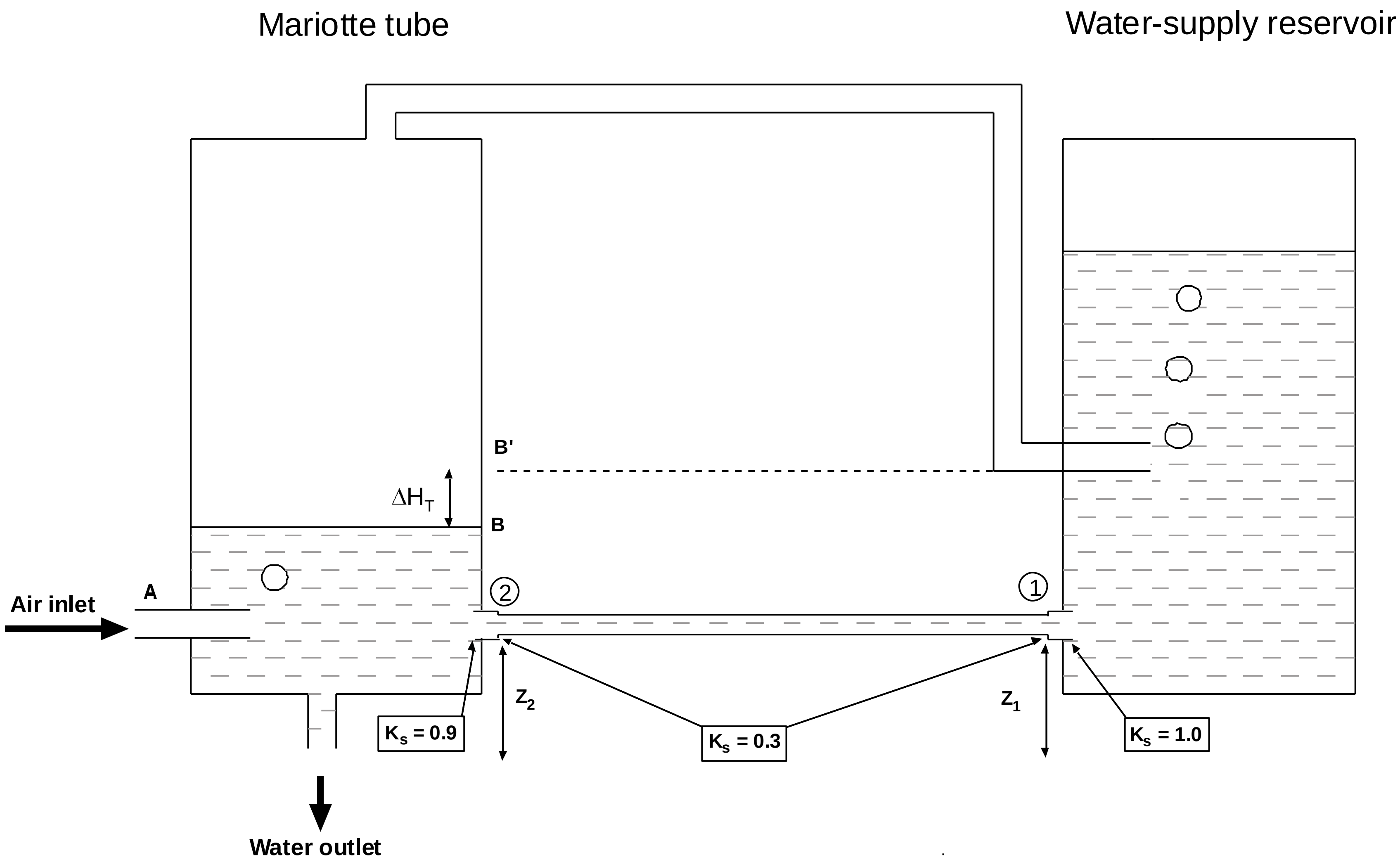

Mariotte tube
Water-supply reservoir
B'
ΔH_T
B
A
Air inlet
2
1
Z2
Z1
Ks = 0.9
Ks = 0.3
Ks = 1.0
Water outlet

Fig. 1

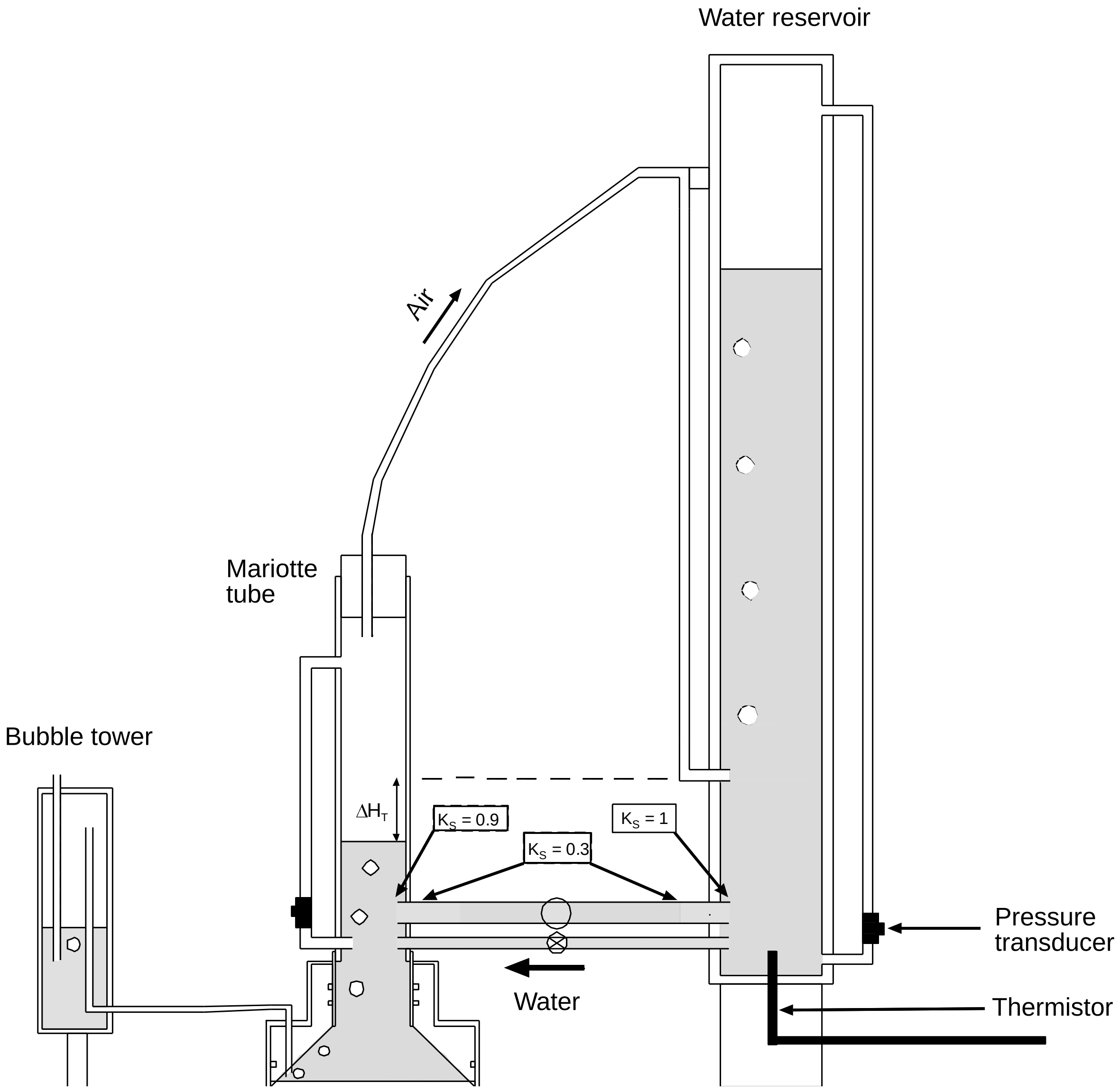
Water reservoir
Air
Mariotte tube
Bubble tower
ΔH_T
K_S = 0.9
K_S = 1
K_S = 0.3
Pressure transducer
Water
Thermistor

Fig. 2.

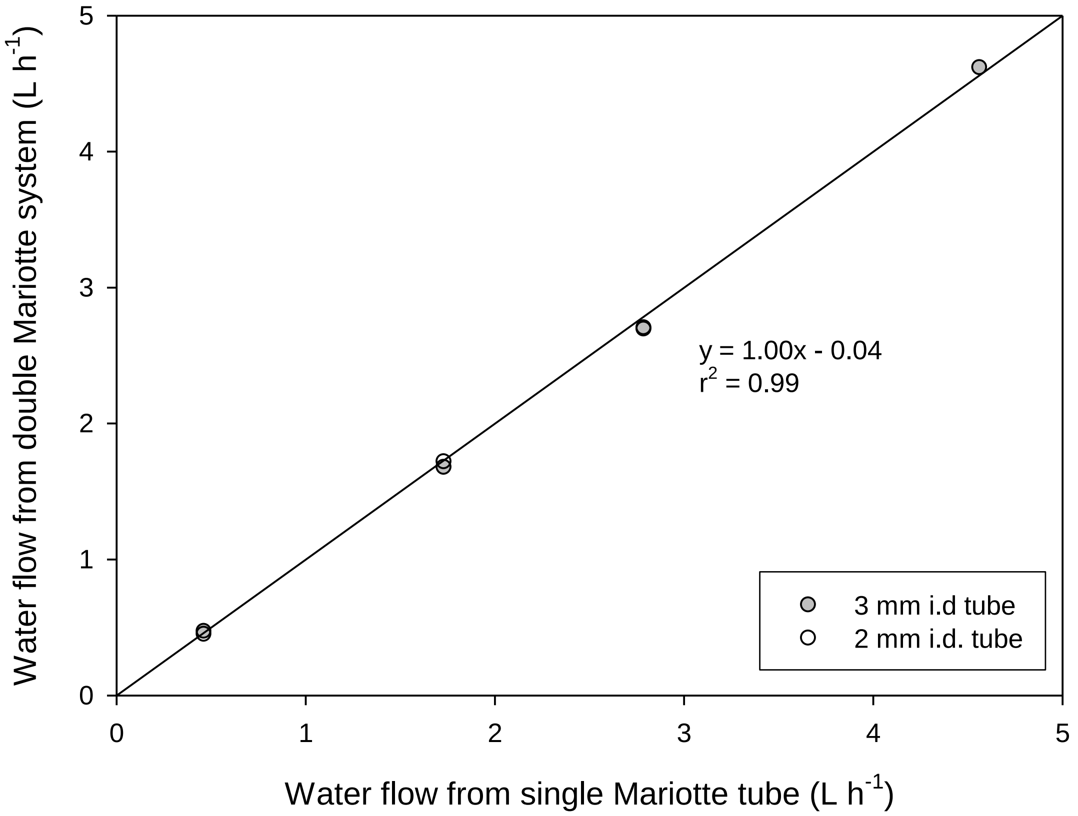
5
4
3
2
1
0
0
1
2
3
4
5
Water flow from double Mariotte system (L h-1)
Water flow from single Mariotte tube (L h-1)
y = 1.00x - 0.04
r2 = 0.99
3 mm i.d tube
2 mm i.d. tube

Fig. 3

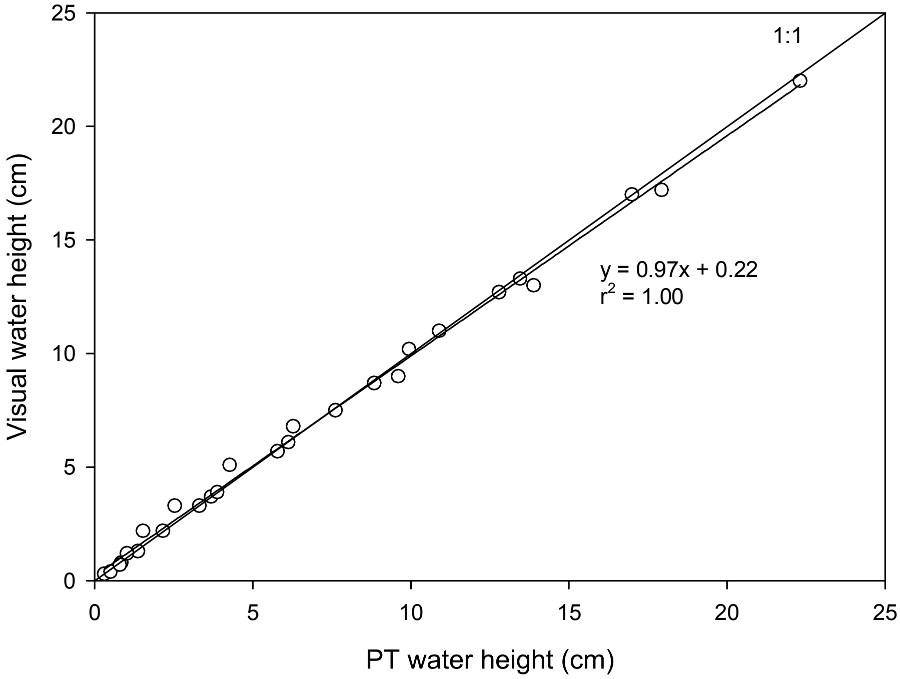
25
20
15
10
5
0
0
5
10
15
20
25
Visual water height (cm)
PT water height (cm)
1:1
y = 0.97x + 0.22
r2 = 1.00

Fig. 4

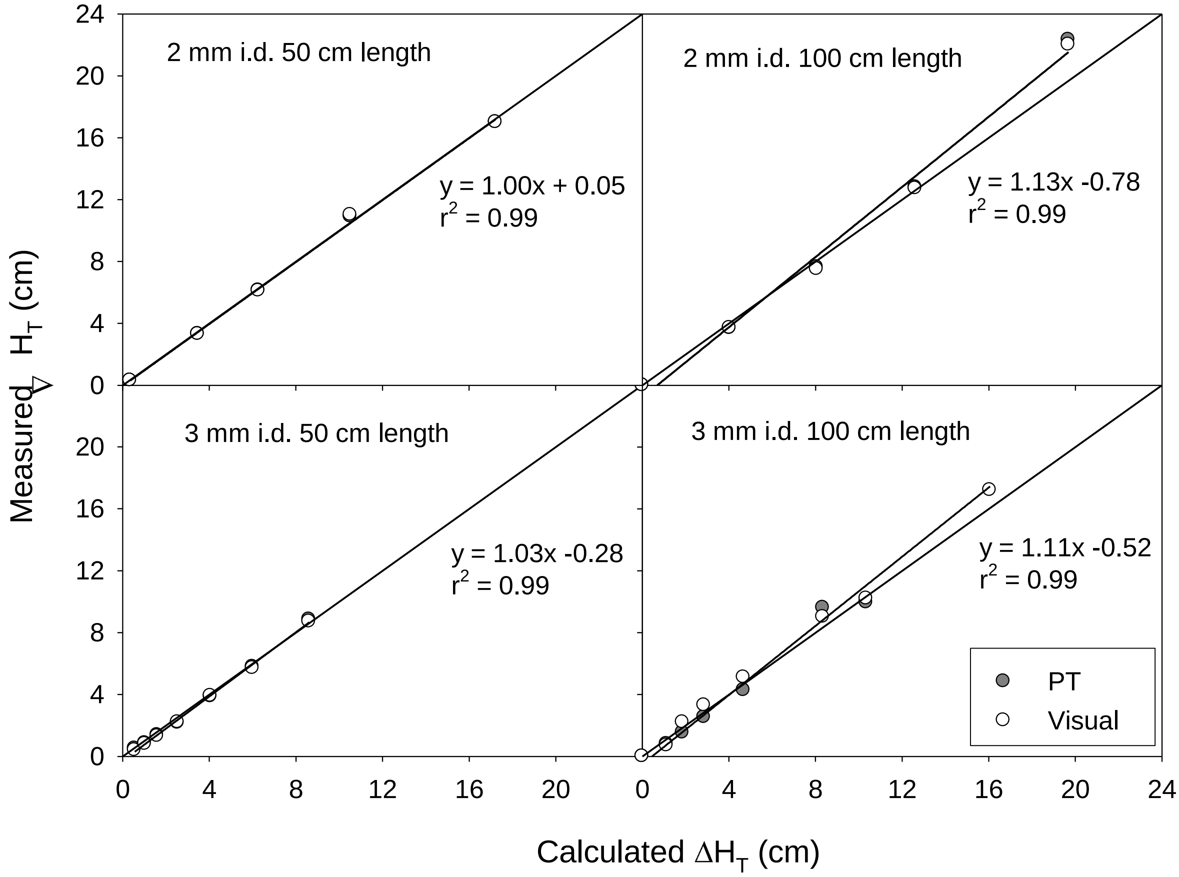

2 mm i.d. 50 cm length
y = 1.00x + 0.05
r2 = 0.99
2 mm i.d. 100 cm length
y = 1.13x -0.78
r2 = 0.99
3 mm i.d. 50 cm length
y = 1.03x -0.28
r2 = 0.99
3 mm i.d. 100 cm length
y = 1.11x -0.52
r2 = 0.99
PT
Visual
Measured ∇ HT (cm)
Calculated ΔHT (cm)
0
4
8
12
16
20
24

Fig. 5.

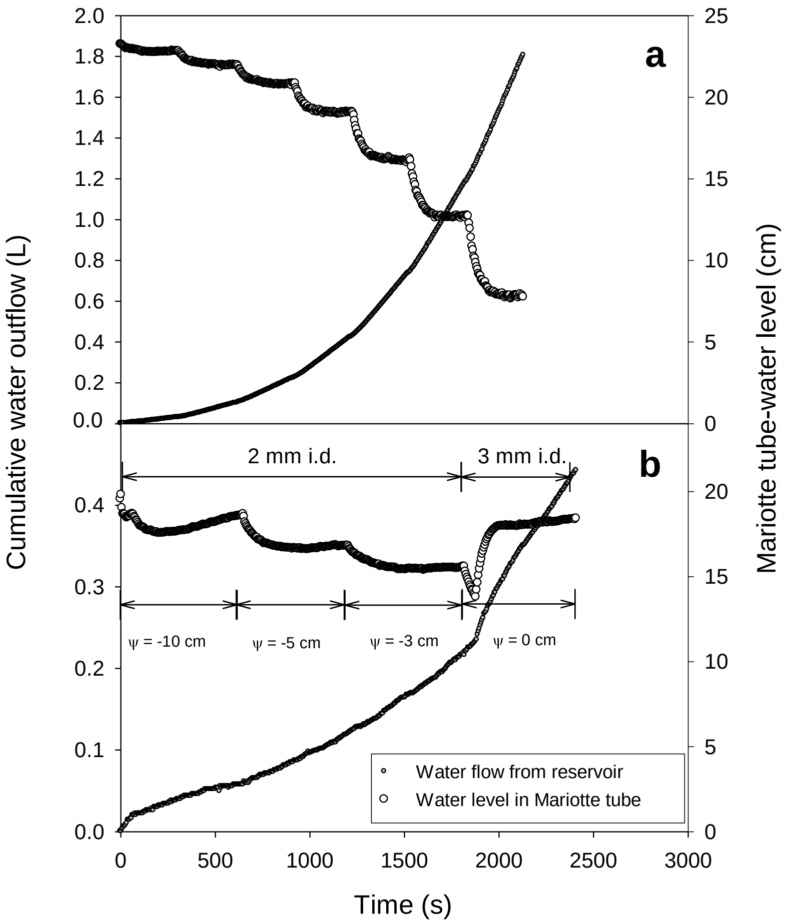

a
b
Cumulative water outflow (L)
Mariotte tube-water level (cm)
Time (s)
2 mm i.d.
3 mm i.d.
ψ = -10 cm
ψ = -5 cm
ψ = -3 cm
ψ = 0 cm
Water flow from reservoir
Water level in Mariotte tube
2.0
1.8
1.6
1.4
1.2
1.0
0.8
0.6
0.4
0.2
0.0
0.3
0.1
25
20
15
10
5
0
0
500
1000
1500
2000
2500
3000

Fig. 6.

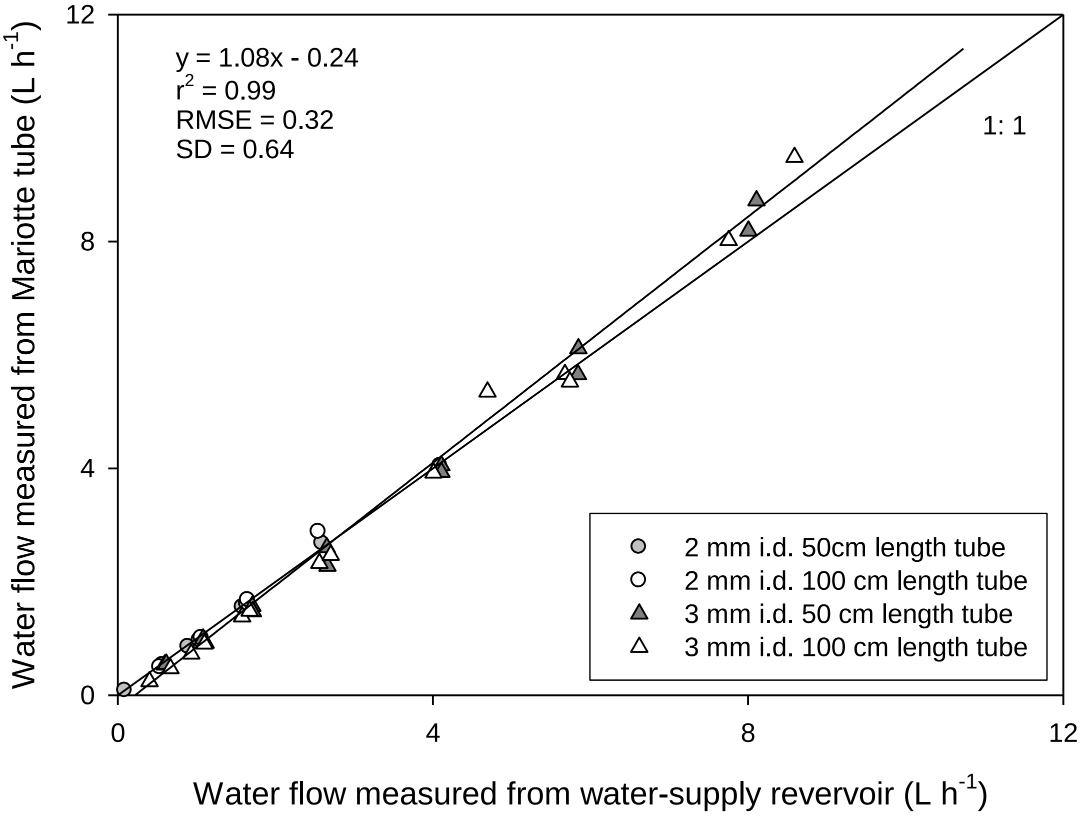
y = 1.08x - 0.24
r2 = 0.99
RMSE = 0.32
SD = 0.64
1: 1
2 mm i.d. 50cm length tube
2 mm i.d. 100 cm length tube
3 mm i.d. 50 cm length tube
3 mm i.d. 100 cm length tube
0
4
8
12
0
4
8
12
Water flow measured from Mariotte tube (L h-1)
Water flow measured from water-supply revervoir (L h-1)

Fig. 7.

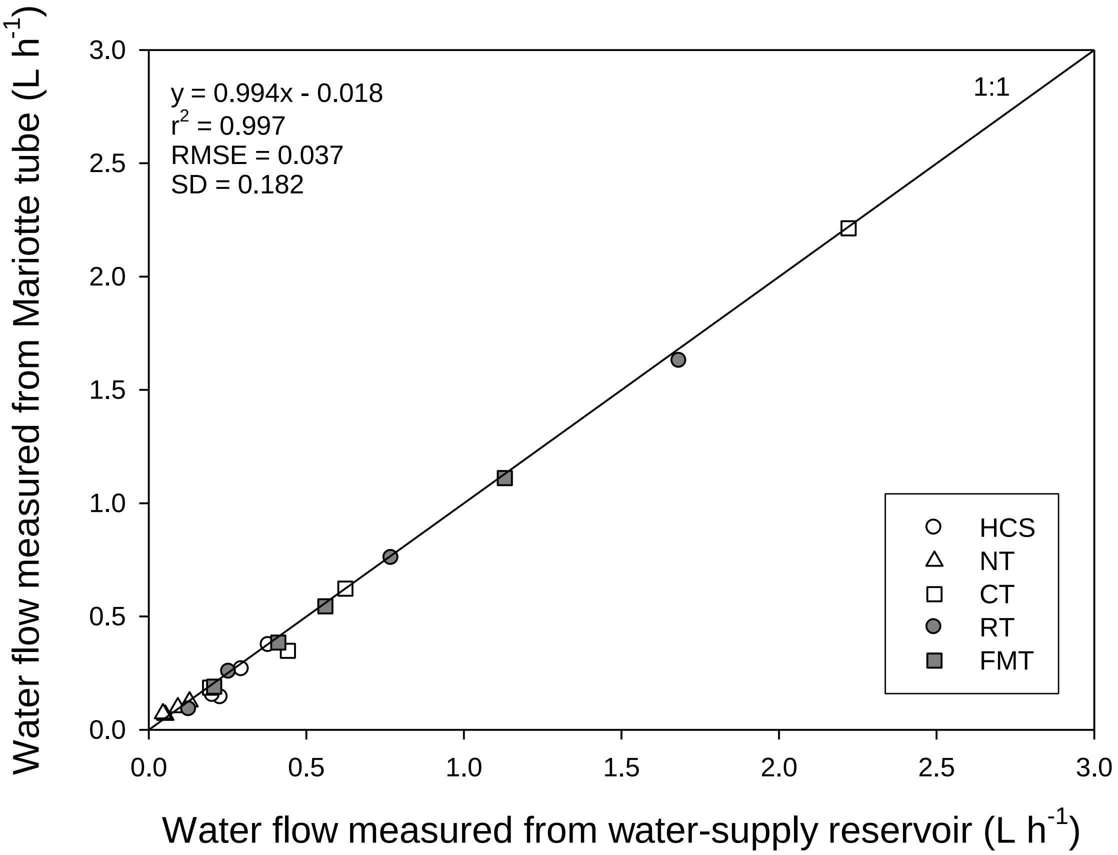
Water flow measured from Mariotte tube (L h-1)
3.0
2.5
2.0
1.5
1.0
0.5
0.0
y = 0.994x - 0.018
r2 = 0.997
RMSE = 0.037
SD = 0.182
1:1
HCS
NT
CT
RT
FMT
0.0
0.5
1.0
1.5
2.0
2.5
3.0
Water flow measured from water-supply reservoir (L h-1)

Fig. 8

Table 1. Effective length and internal diameter (i.d.) for the four different water-flow silicone pipes used in the laboratory and the field experiments.

	Effective length	Effective i.d.
	mm	
2 mm i.d 50 cm length	518.5	2.05
2 mm i.d 100 cm length	1018.5	2.05
3 mm i.d 50 cm length	540.0	2.89
3 mm i.d 100 cm length	1020.2	2.89

Table 2. Characteristics, dry bulk density (ρ_b) and initial volumetric water content (θ_0) of the different soils used to test the new method of water flow measurement applied to the disc infiltrometer, and the supply pressure heads (ψ) applied in the infiltration experiments.

Soil	Observation	ρ_b (g cm^{-3})	θ_0 (cm cm^{-3})	ψ† (cm)
HCS	Highly tractor-compacted loam soil	1.39	0.03	-10 (2), -5 (2), -1 (2), 0 (2)
NT	Loam soil of a long-term conservation tillage experiment (1989-2009) under no tillage management after an 8-month fallow period of a barley-fallow rotation	1.43	0.18	-5 (2), -3 (2), -1 (2), 0 (2)
CT	Loam soil after six months of barley cropping sowed in a soil with a mouldboard plough tillage management	1.25	0.11	-10 (2), -5 (3), -3 (3), 0 (3)
RT	Loam loosened soil after a pass with a rototiller and a 10 mm rainfall	1.12	0.17	-10 (2), -5 (2), -1 (2), 0 (3)
FMT	Freshly mouldboard-tilled loam soil after a pass with a land-roller	1.29	0.13	-10 (2), -5 (2), -3 (2), 0 (3)

†Parenthesis after each supply pressure head indicates the i.d. silicone pipe (Table 1) used for the corresponding supply pressure head in the infiltration experiment

Table 3. Reynolds number (Eq. 5) and continuous (ΔH_C) (Eq. 9), singular (ΔH_S) (Eq. 10) and total (ΔH_T) (Eq. 11) head losses for the first repetition of the laboratory experiment calculated from different water flows running through the 2-and 3-mm internal diameter (i.d.) pipes of 50 and 100 cm length, respectively.

Water flow	Reynolds number	ΔH_C	ΔH_S	ΔH_T
$l\ h^{-1}$		cm		
	3-mm i.d. and 100-cm-long silicone pipe			
0.67	84	1.12	0.01	1.13
1.10	138	1.84	0.03	1.87
1.67	210	2.79	0.06	2.86
2.70	340	4.51	0.17	4.68
4.69	590	7.84	0.51	8.35
5.74	722	9.59	0.76	10.35
8.59	1080	14.35	1.71	16.06
	3-mm i.d. and 50-cm-long silicone pipe			
0.62	74	0.55	0.01	0.56
1.12	134	1.00	0.03	1.03
1.72	206	1.54	0.07	1.60
2.66	319	2.38	0.16	2.54
4.11	493	3.68	0.38	4.06
5.84	701	5.23	0.77	6.00
8.01	960	7.17	1.44	8.61
	2-mm i.d. and 100-cm-long silicone pipe			
0.54	93	4.01	0.03	4.04
1.06	185	7.95	0.11	8.06
1.65	287	12.34	0.27	12.61
2.55	443	19.03	0.65	19.68
	2-mm i.d. and 50-cm-long silicone pipe			
0.09	16	0.35	0.00	0.35
0.89	156	3.40	0.08	3.48
1.58	276	6.02	0.25	6.27
2.59	451	9.85	0.67	10.52
.09	712	15.56	1.67	17.22